Supplement

Podocyte foot process imaging in mouse by fluorescence microscopy

Ivica Grgic, Craig R. Brooks, Andreas F. Hofmeister, Vanesa Bijol, Joseph V. Bonventre, and Benjamin D. Humphreys

Supplemental Video Legends

Video 1

The video shows one whole hemisphere of a DAPI counterstained glomerulus from a tamoxifen-treated bigenic Coll1α1GCE^{+};R26Tomato^{+} mouse. As expected, fate labeled podocytes are mainly located at the outer aspect of the glomerular tuft. Z-stacks of a 50 µm thick mounted kidney section were acquired by confocal microscopy and collected at 1 µm intervals for a total of 49 µm. Nikon NIS elements software was used to recombine z-stacks, obtain a 3D reconstructed image and generate the video.

Video 2

This video shows a 3D reconstruction of a singular genetically labeled podocyte from a DAPI counterstained Coll1α1GCE^{+};R26Tomato^{+} kidney section (5 µm). Z-stacks were collected on a Nikon Eclipse Ti inverted fluorescence microscope at 0.2 µm intervals for a total of 6 µm and recombined using Nikon NIS elements software with an Extended Depth of Focus (EDF) algorithm.

Video 3

This video shows the 3D reconstructed surface of a capillary loop from an anti-laminin immunostained (green) and DAPI counterstained Coll1α1GCE$^+$;R26Tomato$^+$ kidney section (7 µm). Z-stacks were collected on a Nikon Eclipse Ti inverted fluorescence microscope at 0.2 µm intervals and recombined using Nikon NIS elements software with an Extended Depth of Focus (EDF) algorithm.

Supplemental Figure Legends

Supplemental Figure 1

Hypothesis: Sporadic podocyte labeling improves contrast between foot processes. (**A**) The first illustration shows a scenario in which both interdigitating podocytes have undergone a recombination event and therefore express the fluorophor. Filtration slits between labeled foot processes do not provide sufficient contrast to distinguish single pedicles. (**B**) The second illustration shows a scenario in which only one podocyte has been genetically labeled. Each space between two labeled pedicles is now constituted by twice the width of a filtration slit and the width of an unlabeled, optically "silent" foot process, which will increase optical contrast.

Supplemental Figure 2

Probability of visualizing processes of sporadically labeled podocytes in kidney sections of Coll1α1GCE$^+$;R26Tomato$^+$ mice by fluorescence microscopy. A total of 101 glomeruli (with ≥ 1 labeled podocytes) were imaged and evaluated for visibility of primary, secondary and

tertiary FP. The total number of examined podocytes was 432 with an average of 4.3 ± 0.24 labeled podocytes (defined by the presence of a nucleated cell body) per glomerular cross section. Tertiary foot processes could be identified in 290/432 labeled podocytes.

Supplemental Figure 3

Imaging of anti-nephrin, phalloidin and anti-CD31 stained Coll1α1GCE$^+$;R26Tomato$^+$ kidney sections on a tertiary FP level by fluorescence microscopy. (**A**) Anti-nephrin staining demonstrates a close association between labeled tertiary FP (red) and nephrin (green) but fails to resolve single FP. (**B**) Fluorescent phalloidin staining shows a close association of FP (red) with phalloidin-labeled F-actin filaments (green) but is also unsuitable to delineate single tertiary FP in tissue sections by fluorescence microscopy. (**C**) Anti-CD31 staining illustrates the adjacence of podocyte FP (red) and the underlying glomerular capillary endothelium (green), both of which are integral parts of the filtration barrier. Scale bars: 2 μm.

Supplemental Figure 4

Imaging of anti-nephrin and phalloidin stained kidney sections from PS-perfused Coll1α1GCE$^+$;R26Tomato$^+$ mice on a tertiary FP level by fluorescence microscopy. (**A**) Anti-nephrin staining shows that PS-exposed podocyte FP (red) maintain a close association with nephrin (green). (**B**) Fluorescent phalloidin staining demonstrates a strong association between PS-exposed FP (red) and phalloidin-labeled F-actin filaments (green). Some structures exhibit

increased intensities for both signals, potentially consistent with sites of focal FP clubbing/lateralization (arrow heads). Scale bars: 2 μm.

Supplemental Methods

Transgenic mice. Coll1α1GCE (*Collagen1α1-GFP-Cre-ERT2*) transgenic mice were generated using standard techniques; comprehensive details of this line will be documented elsewhere (I.G. and B.D.H., unpublished data). Cre-reporter lines R26LacZ (*Gt(ROSA)26Sor*^{tm1Sor}), mT/mG (*Gt(ROSA) 26Sor*$^{tm4(ACTB\text{-}tdTomato,\text{-}EGFP)Luo}$) and R26Tomato (*Gt(ROSA)26Sor*$^{tm9(CAG\text{-}tdTomato)Hze}$) were obtained from The Jackson Laboratory (Bar Harbor, ME). Coll1α1GCE mice were mated with reporter lines to produce bigenic Coll1α1GCE^{+};R26LacZ^{+}, Coll1α1GCE^{+};mT/mG^{+} mice and Coll1α1GCE^{+};R26Tomato^{+} mice. Genotyping of all mice was performed by PCR.

Tamoxifen/4-hydroxytamoxifen (4-OHT). Tamoxifen (Sigma) or its active metabolite 4-OHT (Sigma) were dissolved in 3% ethanol-containing cornoil (Sigma) at a concentration of 10 mg/mL. Solutions were heated at 45°C for 20-30 min until the compounds were completely dissolved. Pups (P0-P7) were subjected to subcutaneous injection of either tamoxifen/4-OHT (P0: 0.1mg; P3: 0.25mg; P7: 0.5mg) or same volumes of vehicle only. Animals were sacrificed at 6-10 weeks of age.

Mouse kidney perfusion. For induction of foot process effacement mouse kidneys were perfused with protamine sulfate (PS) as described elsewhere [1-3]. Briefly, mice were anesthetized with pentobarbital sodium (60 mg/kg body weight) and placed on a heating pad to maintain the core temperature at 37 °C throughout the procedure. Kidneys were perfused through the left ventricle with solutions maintained at 37 °C at an infusion rate of 9 ml/min. Perfusion was carried out with HBSS for 2 min, followed by protamine sulfate (2 mg/ml in HBSS) for 15 min.

Histological analysis. Kidneys were harvested and processed for histological analyses as previously described [4]. Briefly, mice were sacrificed under deep anesthesia and immediately perfused via the left ventricle with ice-cold PBS for 1 min. Kidneys were hemisectioned, fixed in 4% paraformaldehyde for 1-2 hr at 4°C, cryoprotected in 30% sucrose overnight, and snap-frozen in optimal cutting temperature compound (OCT, Sakura FineTek). Cryosections (5-7μm) were mounted on Fisher Superfrost Plus (Fisher) microscope slides, immunostained if indicated and mounted in ProLong Gold Antifade containing 4′, 6-diamino-2-phenylindole (Invitrogen). LacZ activity was determined by standard X-gal staining and sections counterstained with nuclear fast red solution prior to mounting. FITC-conjugated phalloidin (1:500; Invitrogen) was used to probe for F-actin. The following primary antibodies were used for immunostaining: guinea pig anti-nephrin (1:100; Progen Biotechnik), rat anti-CD31 (1:100; eBioscience), rat anti-PDGFRβ (1:200; eBioscience), and rabbit anti-laminin (1:500; Sigma). Sections were subsequently exposed to corresponding Cy5/DyLight649-conjugated secondary antibodies (Jackson ImmunoResearch).

Imaging and morphometric analysis of podocytes. Mounted kidney sections of 5–7 μm thickness were imaged using a Nikon C1 D-Eclipse confocal microscope or a Nikon Eclipse Ti inverted fluorescence microscope and 60 or 100x objectives. Z-stacks were collected at 0.2 μm intervals for a total of 6-8 μm. To obtain high quality images of foot processes, the z-stacks were processed and recombined using Nikon NIS elements software with an Extended Depth of Focus (EDF) algorithm to obtain a focused or 3D reconstructed image. 10-30 glomeruli were captured per kidney section in a random fashion. Morphometric analyses were performed using Nikon NIS elements software. Podocyte cell body area measurements excluded primary, secondary and tertiary processes. Widths of primary and secondary processes were measured at ≥ 3 different positions and the mean was determined. Lengths of tertiary foot processes were measured from base to tip; widths of tertiary foot processes were measured at the pedicle's apical third.

Statistics. Data are given as mean ± SEM if not otherwise indicated. Statistical analysis was performed using the unpaired Student's *t* test. P values of less than 0.05 were considered statistically significant.

1. Garg P, Verma R, Cook L, Soofi A, Venkatareddy M, George B, Mizuno K, Gurniak C, Witke W, Holzman LB: Actin-depolymerizing factor cofilin-1 is necessary in maintaining mature podocyte architecture. *J Biol Chem* 285**:** 22676-22688, 2010
2. Asanuma K, Kim K, Oh J, Giardino L, Chabanis S, Faul C, Reiser J, Mundel P: Synaptopodin regulates the actin-bundling activity of alpha-actinin in an isoform-specific manner. *J Clin Invest* 115**:** 1188-1198, 2005
3. Verma R, Kovari I, Soofi A, Nihalani D, Patrie K, Holzman LB: Nephrin ectodomain engagement results in Src kinase activation, nephrin phosphorylation, Nck recruitment, and actin polymerization. *J Clin Invest* 116**:** 1346-1359, 2006
4. Humphreys BD, Valerius MT, Kobayashi A, Mugford JW, Soeung S, Duffield JS, McMahon AP, Bonventre JV: Intrinsic epithelial cells repair the kidney after injury. *Cell Stem Cell* 2**:** 284-291, 2008

Supplemental Figure 1

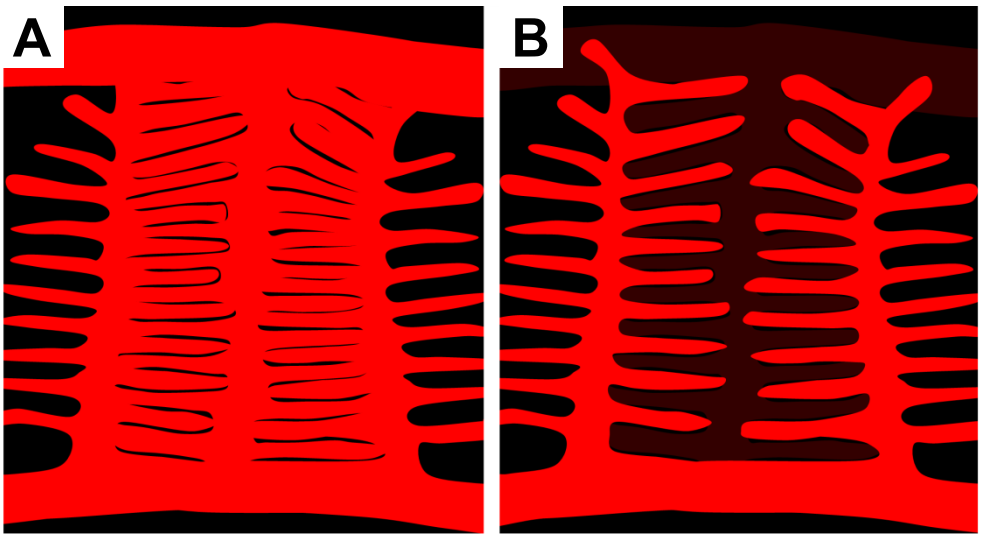

Supplemental Figure 2

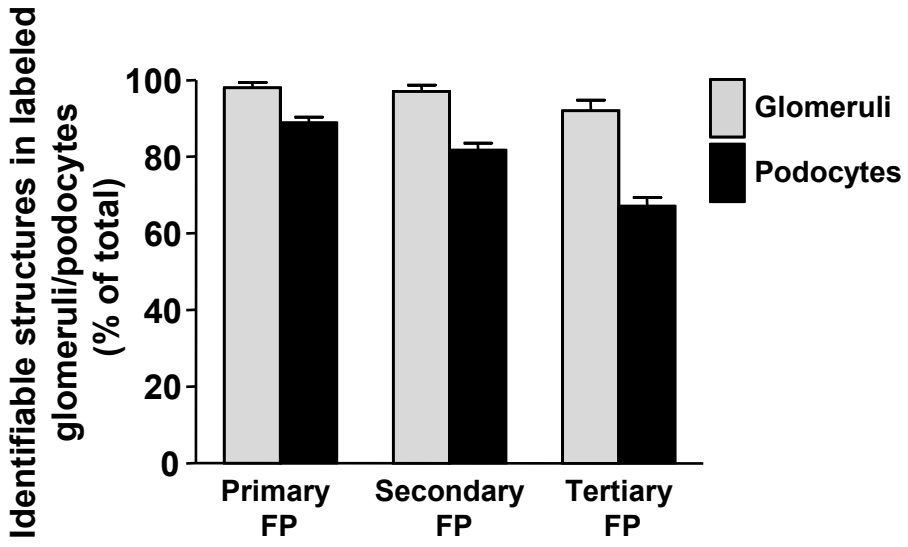

Supplemental Figure 3

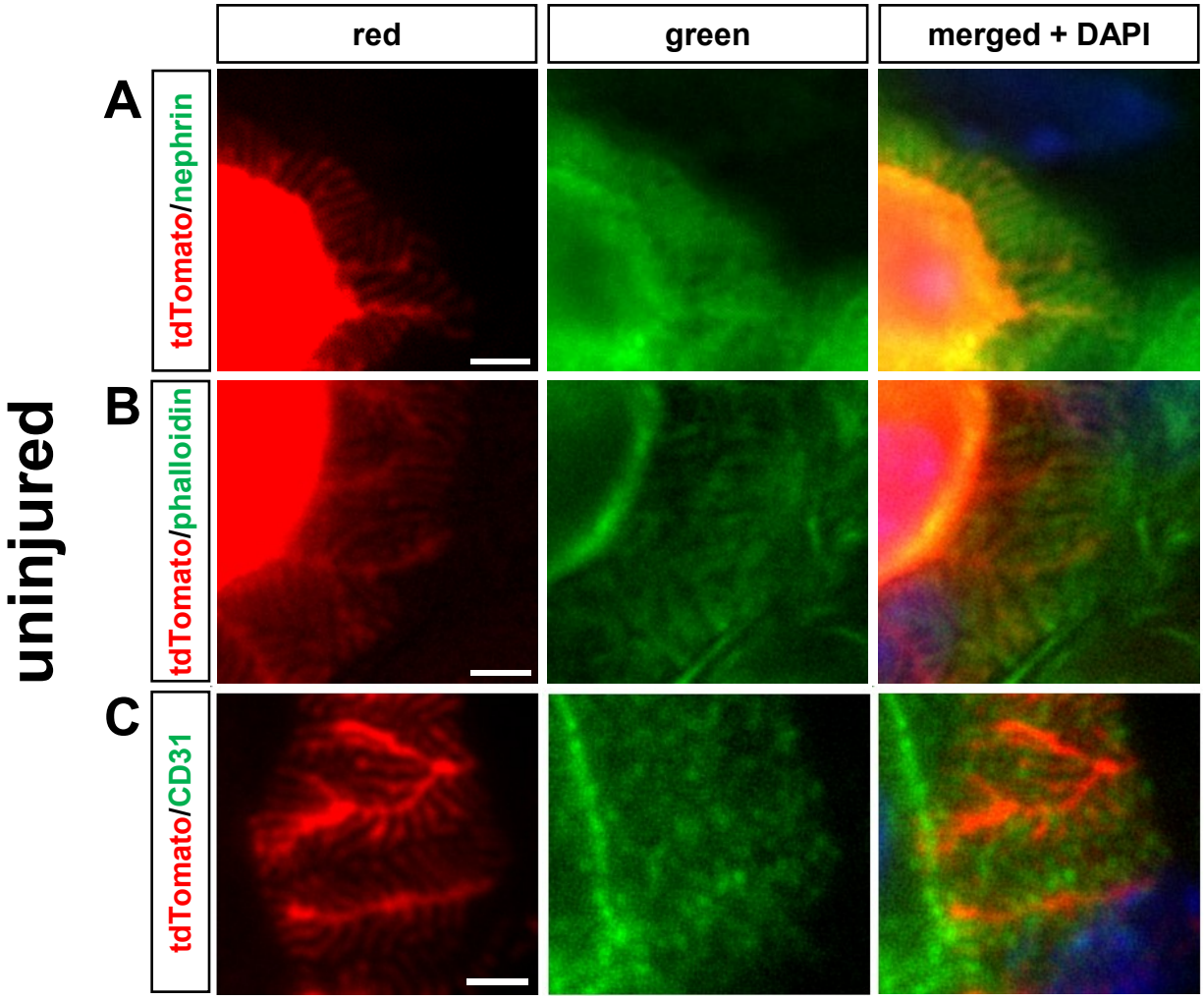
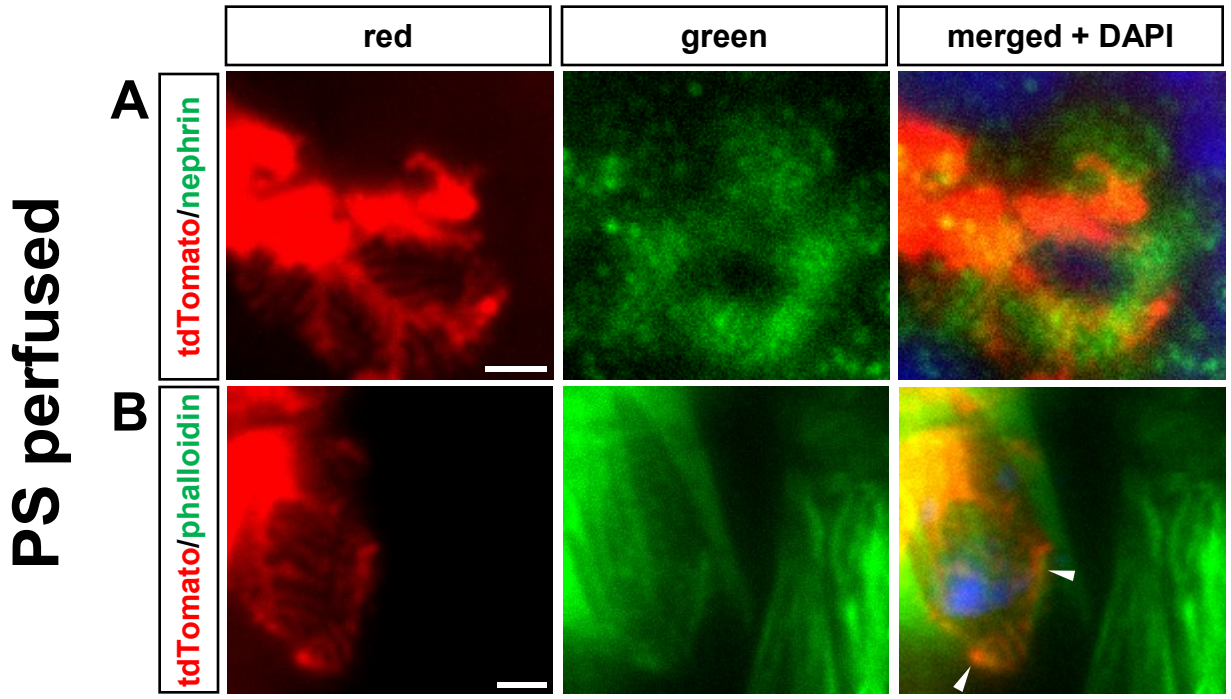
Supplemental Figure 4